INSTITUTE OF PHYSICS PUBLISHING JOURNAL OF PHYSICS: CONDENSED MATTER

J. Phys.: Condens. Matter **17** (2005) S4047–S4058 doi:10.1088/0953-8984/17/49/003

Correlated particle dynamics in concentrated quasi-two-dimensional suspensions

H Diamant[1,3], **B Cui**[2,4], **B Lin**[2] **and S A Rice**[2]

[1] School of Chemistry, Raymond and Beverly Sackler Faculty of Exact Sciences, Tel Aviv University, Tel Aviv 69978, Israel
[2] Department of Chemistry, The James Franck Institute and CARS, The University of Chicago, Chicago, IL 60637, USA

E-mail: hdiamant@tau.ac.il

Received 26 June 2005, in final form 3 August 2005
Published 25 November 2005
Online at stacks.iop.org/JPhysCM/17/S4047

Abstract

We investigate theoretically and experimentally how the hydrodynamically correlated lateral motion of particles in a suspension confined between two surfaces is affected by the suspension concentration. Despite the long range of the correlations (decaying as $1/r^2$ with the inter-particle distance r), the concentration effect is present only at short inter-particle distances for which the static pair correlation is nonuniform. This is in sharp contrast with the effect of hydrodynamic screening in unconfined suspensions, where increasing the concentration changes the prefactor of the large-distance correlation.

(Some figures in this article are in colour only in the electronic version)

1. Introduction

The Brownian motion of colloid particles and macromolecules is correlated through hydrodynamic interactions, i.e., flows that the motion induces in the host liquid [1, 2]. In an unconfined suspension [3] these correlations decay with inter-particle distance r as $1/r$. They are positive, i.e., particles drag one another in the same direction. The long range of the interaction leads to strong many-body effects, manifest in an appreciable dependence of transport coefficients on concentration. A concentration effect of particular interest is hydrodynamic screening [2], which sets in over distances much larger than the inter-particle distance and renormalizes the prefactor of the $\sim 1/r$ pair interaction.

Colloids may sometimes be spatially confined by rigid boundaries, as in porous media, biological constrictions, or microfluidic devices. Attention has been turned recently toward the dynamics of such confined suspensions [4–12] due to the emergence of microfluidic

[3] Author to whom any correspondence should be addressed.
[4] Present address: Department of Physics, Stanford University, Stanford, CA 94305, USA.

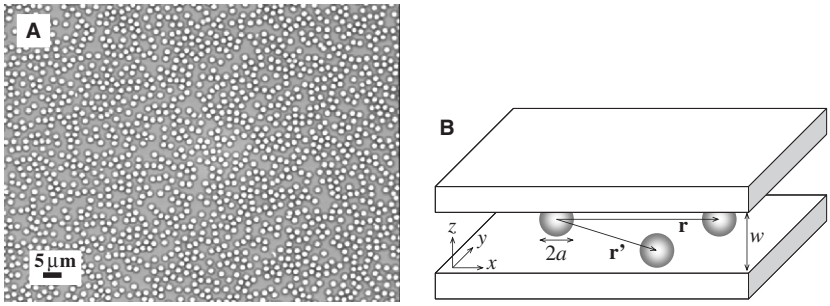

Figure 1. (A) Optical microscope image of the experimental Q2D suspension at area fraction $\phi = 0.338$. (B) Schematic view of the system and its parameters.

applications and the development of new visualization and manipulation techniques (digital video microscopy [13] and optical tweezers [14]), allowing the study of dynamics at the single- and few-particle level. The dynamics of confined suspensions have also been studied by computer simulations [15–17] and there has been renewed interest in related hydrodynamic problems [18, 19].

We have recently demonstrated the dramatic effect that confinement between two flat surfaces has on the hydrodynamic pair interaction at large inter-particle distances [10, 11]. Such a quasi-two-dimensional (Q2D) suspension is portrayed in figure 1. Despite the confinement, the hydrodynamic interaction is still long-range, decaying as $1/r^2$ rather than $1/r$. There is 'anti-drag' in the transverse direction, i.e., the correlation between two particles moving perpendicular to their connecting line is negative. Arguably the most striking finding, however, is that the concentration of the suspension has no effect on the large-distance correlation, i.e., there is no hydrodynamic screening. These three properties are in stark contrast with their unconfined counterparts mentioned above.

In the current paper we review these results and then extend the analysis to shorter inter-particle distances where the static pair correlation of the suspension plays a crucial role. Throughout the paper we present the theoretical analysis along with the corresponding experimental results. Section 2 introduces the model system and the corresponding terminology, and section 3 describes the experimental setup and methods. In section 4 we briefly discuss the dynamics of a single particle and in section 5 address the hydrodynamic interaction between two isolated particles. Section 6, which constitutes the main part of the current work, deals with the three-body correction to the pair interaction at finite concentration. Finally, in section 7 we conclude and discuss the results.

2. Model system

The geometry considered in this work is depicted in figure 1(B). Identical, spherical particles of radius a are suspended in a liquid of viscosity η and temperature T, confined in a slab of width w between two planar solid surfaces. The $\hat{x}$ and $\hat{y}$ axes are taken parallel, and the $\hat{z}$ axis perpendicular, to the surfaces, where $z = 0$ is the mid-plane. The particles behave as hard spheres with no additional equilibrium interaction. For simplicity we consider cases where particle motion is restricted to two dimensions, i.e., to a monolayer lying at the mid-plane. We use the notation $\mathbf{r}(\boldsymbol{\rho}, z)$ for three-dimensional position vectors, where $\boldsymbol{\rho}(x, y)$ is a two-dimensional position vector in the monolayer. The area fraction occupied by particles is denoted by ϕ. The Reynolds number is very low, and the hydrodynamics, therefore, are well

described by viscous Stokes flows [3]. The confining boundaries are impermeable and rigid, imposing no-slip boundary conditions on the flow.

We characterize the dynamic pair correlation between two particles by the coupling mobilities $B^{\rm c}_{\rm L,T}(\rho)$ as functions of the inter-particle distance ρ. These are the off-diagonal terms in the mobility tensor of a particle pair, i.e., the proportionality coefficients relating the force acting on one particle with the change in velocity of the other. The two independent coefficients, $B^{\rm c}_{\rm L}$ and $B^{\rm c}_{\rm T}$, correspond, respectively, to the coupling along and transverse to the line connecting the pair. The dynamic correlation between two Brownian particles is similarly characterized by two coupling diffusion coefficients, $D^{\rm c}_{\rm L,T}(\rho)$, which, due to the Einstein relation, are simply related to the coupling mobility coefficients via the thermal energy, $D^{\rm c}_{\rm L,T}(\rho) = k_{\rm B}T\,B^{\rm c}_{\rm L,T}(\rho)$. (In [10] four coefficients were considered, $D^{\pm}_{\rm L,T}$, whose relation with the ones considered here is $D^{\rm c}_{\rm L,T} = (D^{+}_{\rm L,T} - D^{-}_{\rm L,T})/2$.)

3. Experimental setup

The experimental system consists of an aqueous suspension of monodisperse silica spheres (diameter $2a = 1.58 \pm 0.04$ μm, density 2.2 g cm^{-3}, Duke Scientific), undergoing Brownian motion while being tightly confined between two parallel glass plates in a sealed thin cell (figure 1). The inter-plate separation is $w = 1.76 \pm 0.05$ μm, i.e., slightly larger than the sphere diameter, $2a/w \simeq 0.90$. Digital video microscopy and subsequent data analysis are used to locate the centres of the spheres in the field of view and then extract time-dependent two-dimensional trajectories. Details of the setup and measurement methods can be found elsewhere [20]. Measurements were made at four values of area fraction, $\phi = 0.254$, 0.338, 0.547, 0.619 ± 0.001. (Larger area fractions could not be checked because the suspension began to crystallize [21].) From equilibrium studies of this system [21] we infer that, for the purpose of this study, the particles can be regarded as hard spheres.

The coupling diffusion coefficients as functions of the inter-particle distance are directly measured from the tracked trajectories as

$$D^{\rm c}_{\rm L}(\rho) = \langle x_1(t)x_2(t)\rangle_\rho/(2t), \qquad D^{\rm c}_{\rm T}(\rho) = \langle y_1(t)y_2(t)\rangle_\rho/(2t), \tag{1}$$

where $x_i(t)$ and $y_i(t)$ are the displacements of particle i of the pair during a time interval t along and transverse to their connecting line, respectively. The average $\langle\rangle_\rho$ is taken over all pairs whose mutual distance falls in a narrow range (± 0.09 μm) around ρ.

4. Single particle

Consider a single particle whose centre, lying on the mid-plane between the two confining surfaces, is defined as the origin. A force $\mathbf{f}_1$ is applied to the particle in the i direction parallel to the surfaces ($i = x, y$). As a result, the particle moves with velocity

$$u_{1i} = B_{\rm s} f_{1i} = B_0[(a/w)\Delta_{\rm s}(a/w)]f_{1i}, \tag{2}$$

where $B_{\rm s}$ is the self-mobility of the particle in the given geometry and $B_0 = (6\pi\eta a)^{-1}$ is its self-mobility in an unconfined liquid. Alternatively, we may consider a free Brownian particle. Its mean-square displacement during a time interval t will be

$$\langle\rho^2(t)\rangle = 4D_0[(a/w)\Delta_{\rm s}(a/w)]t, \tag{3}$$

where $D_0 = k_{\rm B}T\,B_0$. The dimensionless factor $(a/w)\Delta_{\rm s}(a/w)$, representing the effect of confinement, becomes unity in the limit $a/w \ll 1$. Approximate expressions for this factor

for larger values of the confinement ratio a/w were the subject of many previous works (see [3] and references therein), and their validity has been confirmed in recent experiments [6–8].

The particle motion makes the surrounding liquid flow. At distances much larger than w the flow velocity is given by [10, 11, 18]

$$\begin{aligned} v_i(\mathbf{r}) &= (a/w)B_0\Delta_{ij}(\mathbf{r})f_{1j} \\ \Delta_{ij}(\boldsymbol{\rho},z) &= -\lambda_0\frac{w^2}{\rho^2}\left(\delta_{ij}-\frac{2\rho_i\rho_j}{\rho^2}\right)H(z/w), \end{aligned} \tag{4}$$

where $i,j = x,y$, the vertical component v_z is exponentially small in ρ/w, and λ_0 is a dimensionless prefactor of order 1 dependent only on the confinement ratio a/w. The flow field (4) can be viewed as produced by an effective two-dimensional mass dipole (source doublet), located at the particle centre and oriented in the j direction [18, 22, 10, 11]. The flow has a perpendicular profile $H(z/w)$ which vanishes on the two confining surfaces, $H(-1/2) = H(1/2) = 0$, and is normalized to 1 at the mid-plane, $H(0) = 1$.

As argued in [10, 11], the far flow has the dipolar shape (4) regardless of particle size. Changing the confinement ratio a/w merely modifies the effective mass-dipole strength, i.e., the prefactor $\lambda_0(a/w)$. In the limit $a/w \to 0$ one finds $\lambda_0 = 9/16$ [18]. As will be shown below, we find for $a/w \simeq 0.45$ that $\lambda_0 \simeq 0.49$. Since the maximum possible confinement ratio is $a/w = 1/2$, it is inferred that the function $\lambda_0(a/w)$ actually changes very little with a/w. This weak dependence on the confinement ratio can be understood in terms of mutual compensation of two opposing effects: when a/w is larger, on the one hand, the particle displaces a larger liquid volume as it moves, yet, on the other hand, its self-mobility decreases (i.e., $(a/w)\Delta_s(a/w)$ gets smaller).

5. Pair interaction

Let us introduce a second particle whose centre lies at $\mathbf{r} = (\boldsymbol{\rho}, 0)$. The particle is torque free. It is also force free in the xy plane. Being confined to the mid-plane, it evidently cannot be assumed force free in the z direction. However, the flow (4) does not exert any force in that direction on a mid-plane-placed particle. Hence, as long as we restrict the discussion to such flows, the particle can be regarded as force free. It is thus entrained by the flow with velocity [3]

$$u_{2i} = \frac{1}{4\pi a^2}\int_A \mathrm{d}\mathbf{r}''\, v_i(\mathbf{r}'') = \left(1-\frac{4a^2}{3w^2}\right)v_i(\boldsymbol{\rho},0), \tag{5}$$

where the integration is over the particle surface A. In obtaining the last equality we have assumed a parabolic (Poiseuille) vertical profile, $H(z/w) = 1-4z^2/w^2$ [18]. Equation (5) is, in fact, a manifestation of Faxen's first law [3] as applied to the Q2D geometry. For a force-free particle, Faxen's law yields $\mathbf{u} = \mathbf{v} + (a^2/6)\nabla^2\mathbf{v}$. The dipolar flow (4) has $(\partial_{xx}+\partial_{yy})\mathbf{v} = 0$ and $\partial_{zz}|_{z=0}\mathbf{v} = [w^{-2}H''(0)/H(0)]\mathbf{v}$, from which equation (5) readily follows.

Substituting equation (4) in (5), we obtain a relation between the force $\mathbf{f}_1$ exerted on the first particle and the resulting velocity change $\mathbf{u}_2$ of the second particle,

$$u_{2i} = [1-4a^2/(3w^2)](a/w)B_0\Delta_{ij}(\boldsymbol{\rho},0)f_{1j}, \tag{6}$$

thus identifying the off-diagonal coupling terms of the pair mobility tensor as $B^c_{ij}(\boldsymbol{\rho}) = [1-4a^2/(3w^2)](a/w)B_0\Delta_{ij}(\boldsymbol{\rho},0)$. To get the coupling mobility along the line connecting the pair, we consider the relation between f_{1x} and u_{2x} for $\boldsymbol{\rho} = \rho\hat{x}$. Using equation (4) we get

$$\begin{aligned} B^c_L(\rho) &= [1-4a^2/(3w^2)](a/w)B_0\Delta_{xx}(\rho\hat{x},0) = (a/w)B_0\Delta_L(\rho) \\ \Delta_L(\rho) &= \lambda w^2/\rho^2. \end{aligned} \tag{7}$$

Similarly, for $\boldsymbol{\rho} = \rho\hat{y}$ the relation between f_{1x} and u_{2x} yields the coupling mobility transverse to the connecting line,

$$\begin{aligned} B^{\mathrm{c}}_{\mathrm{T}}(\rho) &= [1 - 4a^2/(3w^2)](a/w)B_0\Delta_{xx}(\rho\hat{y}, 0) = (a/w)B_0\Delta_{\mathrm{T}}(\rho) \\ \Delta_{\mathrm{T}}(\rho) &= -\lambda w^2/\rho^2. \end{aligned} \tag{8}$$

In equations (7) and (8) we have defined

$$\lambda(a/w) = [1 - 4a^2/(3w^2)]\lambda_0(a/w). \tag{9}$$

This is a refinement of our previous analysis [10, 11]. In a Q2D geometry the so-called stokeslet approximation, equating the coupling mobility with the flow velocity per unit force, strictly holds only when a is much smaller than *both* the inter-particle distance ρ and the slab width w, whereupon $\lambda \simeq \lambda_0 \simeq 9/16$. If a is much smaller than ρ but comparable to w then, no matter how large the inter-particle distance may be, we have $\lambda < \lambda_0$. This is due to the second term in Faxen's law, $\sim a^2\nabla^2\mathbf{v}$. In an unconfined liquid it contributes a negligible correction to the stokeslet limit, $\mathrm{O}(a^2/r^2)$, whereas in Q2D the newly introduced length w leads to a significant correction of $\mathrm{O}(a^2/w^2)$.

As found in equations (7) and (8), the pair hydrodynamic interaction in Q2D is very different from its unconfined counterpart. The decay with distance is faster, $\sim 1/r^2$ instead of $\sim 1/r$, yet the interaction is still long-range [23, 22]. (Its decay, in fact, is *slower* than near a single surface, where the interaction falls off as $1/r^3$ [4, 5].) The transverse coupling is negative, i.e., particles exert 'anti-drag' on one another as they move perpendicular to their connecting line. (In the unconfined case one has $\Delta_{\mathrm{T}} = \Delta_{\mathrm{L}}/2$, both coefficients being positive.) These properties are direct consequences of the far-flow field (4). The $1/\rho^2$ decay is that of the flow due to a 2D mass dipole. The negative transverse coupling is a result of circulation flows in the dipolar field [10].

For a pair of force-free Brownian particles, the hydrodynamic coupling derived above implies that their motions be correlated according to equation (1), with $D^{\mathrm{c}}_{\mathrm{L,T}}(\rho) = (a/w)D_0\Delta_{\mathrm{L,T}}(\rho)$. Thus, the dimensionless couplings $\Delta_{\mathrm{L,T}}(\rho)$ can be directly measured from the statistics of particle trajectories. These measurements for different area fractions ϕ are presented in figure 2. The large-distance behaviour for all ϕ values fits well the $\pm\lambda w^2/\rho^2$ dependence of equations (7) and (8) with $\lambda \simeq 0.36$. The negative sign of Δ_{T} confirms the predicted 'anti-drag' between particles located transverse to the direction of motion. Substituting $\lambda \simeq 0.36$ and $a/w \simeq 0.45$ in equation (9), we find $\lambda_0(0.45) \simeq 0.49$, which is only slightly smaller than the value for a vanishing confinement ratio, $\lambda_0(0) = 9/16 \simeq 0.56$.

6. Concentration effect

As the area fraction ϕ is increased, the pair hydrodynamic interaction should become affected by the presence of other particles. In unconfined suspensions hydrodynamic screening sets in at distances much larger than the typical inter-particle distance and renormalizes the interaction by a concentration-dependent prefactor [2]. Similarly, one expects the pair interaction in Q2D to have the form of equations (7) and (8) yet with a modified, ϕ-dependent prefactor. We find, however, that this is not the case, as is clearly demonstrated in figure 2(e).

Consider again particle 1, located at the origin and exerting a force $\mathbf{f}_1$ parallel to the confining surfaces. This creates a far-flow velocity $\mathbf{v}$ according to equation (4) which, in the absence of any other particle, entrains particle 2 at $\mathbf{r} = (\boldsymbol{\rho}, 0)$ with velocity $\mathbf{u}_2 \sim \mathbf{v}(\mathbf{r})$ given by equation (6). We now introduce particle 3 at $\mathbf{r}' = (\boldsymbol{\rho}', 0)$. It obstructs the flow and thus modifies $\mathbf{u}_2$.

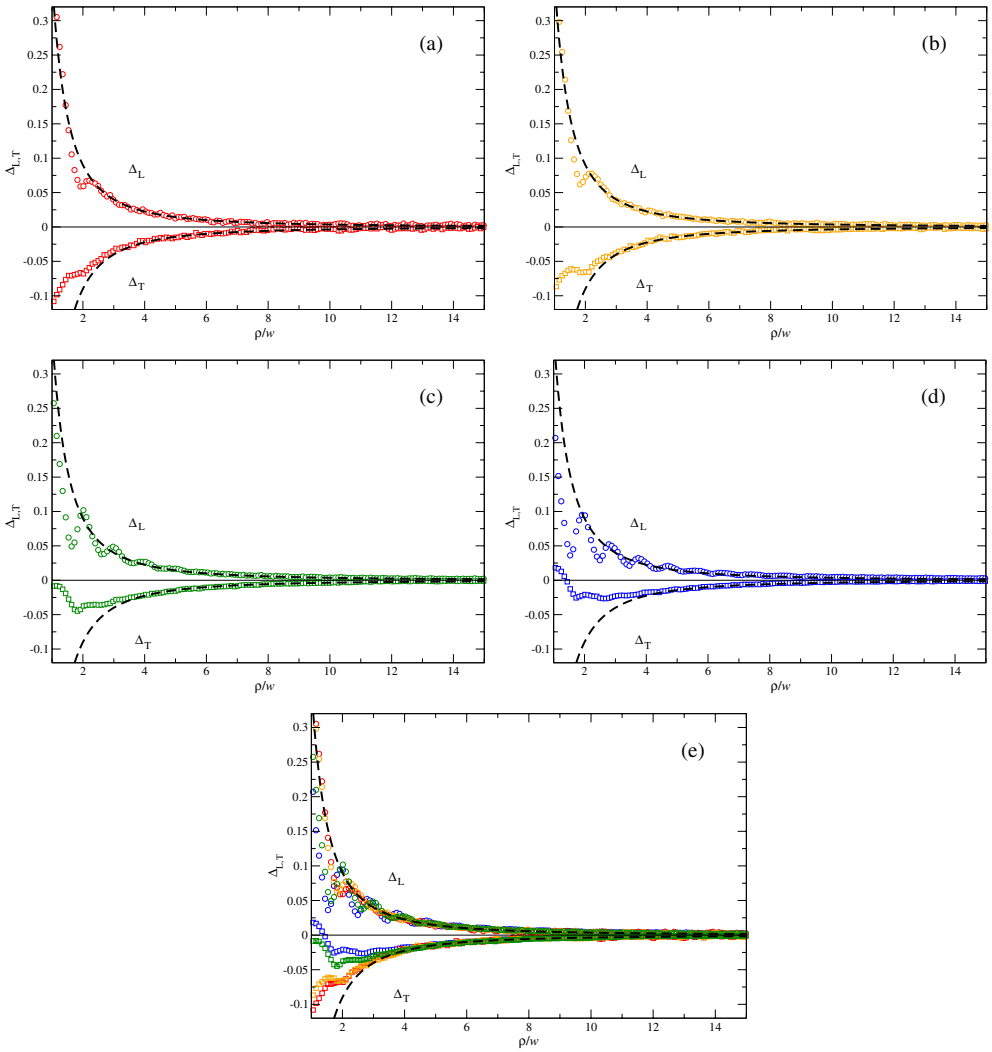

Figure 2. Longitudinal (Δ_L, circles) and transverse (Δ_T, squares) coupling diffusion coefficients as a function of inter-particle distance ρ. The coefficients are scaled by $D_0 a/w$ and the distance by w. Area fractions are $\phi = 0.254$ ((a), red), 0.338 ((b), orange), 0.547 ((c), green), and 0.619 ((d), blue). All data are redrawn in (e), demonstrating a concentration-independent collapse of the large-distance measurements onto the same two curves. Dashed lines are a fit to $\pm\lambda/(\rho/w)^2$ with the same value of $\lambda = 0.36$ for all panels.

The particle being force free, the lowest force-distribution moment it can exert is a force dipole,

$$S_{ij}(\mathbf{r}') = \lambda_s (a/wB_0)^{-1} \frac{1}{4\pi a^2} \int_A \mathrm{d}\mathbf{r}''\, (\mathbf{r}'' - \mathbf{r}')_i v_j(\mathbf{r}''), \tag{10}$$

where the integration is over the surface of particle 3, and λ_s is a dimensionless factor of order 1. The force dipole, located at $\mathbf{r}'$, changes the flow velocity at $\mathbf{r}$ by

$$\delta v_i^s(\mathbf{r}, \mathbf{r}') = S_{jk}(\mathbf{r}')(a/wB_0)\partial_j \Delta_{ki}(\mathbf{r} - \mathbf{r}'). \tag{11}$$

This holds regardless of confinement. In an unconfined system the far flows decay as $1/r$,

leading to $S \sim (r')^{-2}$ and $\delta v^s \sim (r')^{-2}|\mathbf{r} - \mathbf{r}'|^{-2}$. Then, upon integration over the third-particle position $\mathbf{r}'$, one gets a correction $\sim 1/r$, which renormalizes the coefficient of the bare $1/r$ interaction. In Q2D, however, the situation is different. First, we realize that, due to the vanishing of v_z and the symmetry of the mid-plane, only the terms $i, j = x, y$ of S_{ij} in equation (10) are nonzero. Then, since the far flows decay as $1/\rho^2$, one gets $\delta v^s \sim (\rho')^{-3}|\boldsymbol{\rho} - \boldsymbol{\rho}'|^{-3}$ which, upon integration over $\boldsymbol{\rho}'$, yields a correction $\sim 1/\rho^4$. At large distances this is much smaller than the bare pair interaction ($\sim 1/\rho^2$) and will be neglected.

Since the force dipole created by particle 3 has a negligible far-field effect in Q2D, we proceed to the third moment of the force distribution,

$$T_{ijk}(\mathbf{r}') = \lambda_t (a/wB_0)^{-1} \frac{1}{4\pi a^2} \int_A \mathrm{d}\mathbf{r}'' \, (\mathbf{r}'' - \mathbf{r}')_i (\mathbf{r}'' - \mathbf{r}')_j v_k(\mathbf{r}''), \tag{12}$$

where λ_t is another dimensionless prefactor depending only on the confinement ratio a/w. In principle, λ_t (and λ_s) could be calculated using the *short-range* hydrodynamics in a Q2D geometry [18, 19], yet we shall not pursue this technically complicated calculation here. The vanishing of v_z and the mid-plane symmetry make all terms T_{ijk}, for which one or three of the indices are z, vanish. In addition, the terms with $(i, j, k) = (x, y)$ are negligible at large distances compared to those with two z indices, since they involve two additional powers of $1/\rho'$. We are thus left with T_{zzi}, $i = (x, y)$, yielding through equations (4) and (12)

$$T_{zzi}(\boldsymbol{\rho}') = \frac{1}{3}\lambda_t a^2 \left(1 - \frac{12a^2}{5w^2}\right) \Delta_{ij}(\boldsymbol{\rho}', 0) f_{1j}. \tag{13}$$

In the integration we have assumed again a parabolic vertical profile, $H(z/w) = 1 - 4z^2/w^2$ [18]. Note that within this assumption the similar leading terms in $1/\rho'$ from all higher moments of the force distribution, involving higher z derivatives, vanish. The moment $T(\boldsymbol{\rho}')$ changes the flow velocity at $\boldsymbol{\rho}$ by

$$\delta v_i^t(\mathbf{r}, \mathbf{r}') = T_{zzj}(\boldsymbol{\rho}')(a/wB_0)\partial_{zz}|_{z=0} \Delta_{ji}(\boldsymbol{\rho} - \boldsymbol{\rho}', 0). \tag{14}$$

Combining equations (4), (5), (13) and (14), we find the correction to the velocity of particle 2 due to particle 3,

$$\begin{aligned} \delta u_{2i} &= (a/wB_0) C_1 \Delta_{ij}(\boldsymbol{\rho} - \boldsymbol{\rho}') \Delta_{jk}(\boldsymbol{\rho}') f_{1k} \\ C_1 &= -\lambda_t \frac{8a^2}{3w^2} \left(1 - \frac{4a^2}{3w^2}\right) \left(1 - \frac{12a^2}{5w^2}\right), \end{aligned} \tag{15}$$

where the reference to $z = 0$ is hereafter omitted for brevity.

Equation (15) yields the correction to $\mathbf{u}_2$ given a certain position $\boldsymbol{\rho}'$ of particle 3. We now wish to average this correction over all possible $\boldsymbol{\rho}'$,

$$\langle \delta \mathbf{u}_2 \rangle = \int \mathrm{d}^2\rho' \, p(\boldsymbol{\rho}, \boldsymbol{\rho}') \delta \mathbf{u}_2(\boldsymbol{\rho}, \boldsymbol{\rho}'), \tag{16}$$

where $p(\boldsymbol{\rho}, \boldsymbol{\rho}')$ is the probability density of finding particle 3 at $\boldsymbol{\rho}'$ given that particle 2 is at $\boldsymbol{\rho}$ and particle 1 is at the origin. Employing the superposition approximation, we take this probability as

$$p(\boldsymbol{\rho}, \boldsymbol{\rho}') \simeq \frac{\phi}{\pi a^2} g(\rho') g(|\boldsymbol{\rho} - \boldsymbol{\rho}'|) \simeq \frac{\phi}{\pi a^2} [1 + h(\rho') + h(|\boldsymbol{\rho} - \boldsymbol{\rho}'|)], \tag{17}$$

where $g(\rho)$ is the pair correlation function of the Q2D suspension (normalized to 1 at $\rho \to \infty$), and $h(\rho) = g(\rho) - 1$. We have assumed that the monolayer of particles is a disordered 2D liquid, and thus the pair correlation has no angular dependence.

Using equations (15)–(17), and specializing to the relation between $\langle \delta u_{2x} \rangle$ and f_{1x}, we obtain the average corrections to the coupling mobilities,

$$\delta B^{c}_{\mathrm{L,T}}(\rho) = (a/w) B_0 \delta \Delta_{\mathrm{L,T}}(\rho)$$
$$\delta \Delta_{\mathrm{L,T}}(\rho) = (\pi a^2)^{-1} C_1 \phi \int \mathrm{d}^2\rho' \, [1 + 2h(\rho')][\Delta_{xx}(\boldsymbol{\rho} - \boldsymbol{\rho}')\Delta_{xx}(\boldsymbol{\rho}') + \Delta_{xy}(\boldsymbol{\rho} - \boldsymbol{\rho}')\Delta_{xy}(\boldsymbol{\rho}')], \tag{18}$$

where the longitudinal and transverse couplings are obtained, as in section 5, by taking $\boldsymbol{\rho} = \rho\hat{x}$ and $\boldsymbol{\rho} = \rho\hat{y}$, respectively. (Note that equation (18), for $h(\rho) = 0$, has exactly the same form as the one used in [10, 11] based on a less detailed analysis.)

A brief examination of equation (18) raises two expectations. First, the integrand scales as $(\rho')^{-2}|\boldsymbol{\rho} - \boldsymbol{\rho}'|^{-2}$ which, upon integration over $\boldsymbol{\rho}'$, is expected to yield a correction $\sim 1/\rho^2$, i.e., a renormalization of the prefactor of the bare coupling in accord with hydrodynamic screening. Second, since the fields Δ_{ij} decay slowly with distance, one expects features (oscillations) in the static correlation function $h(\rho)$ to be smoothed by integration and thus be manifest only weakly in the dynamic coupling. As is shown below, due to the unique shape of the far flow in Q2D, both of these expectations turn out to be false.

The convolution integral of equation (18) is worked out in the appendix. The result is

$$\delta \Delta_{\mathrm{L,T}}(\rho) = C\phi w^2 \left[\frac{h(\rho)}{\rho^2} - 2 \int_{\rho}^{\infty} \mathrm{d}\xi \, \frac{h(\xi)}{\xi^3} + \mathrm{O}(a^2/\rho^4) \right], \tag{19}$$

where $C = -2(w^2/a^2)\lambda_0^2 C_1$, and the results for the longitudinal and transverse couplings are identical. Equation (19) is the main result of the current work. It gives the leading three-body correction to the pair hydrodynamic interaction in Q2D. If static pair correlations are neglected, $h(\rho) = 0$, this correction *vanishes*, as was presented in [10, 11]. Moreover, the correction for a nonzero $h(\rho)$, although finite, is short-range: since the suspension is disordered, the static pair correlation $h(\rho)$ decays exponentially beyond an equilibrium correlation length. Thus, the correction in equation (19) decreases with distance much faster than the $1/\rho^2$ decay of the bare interaction. This remarkable disagreement with the usual notion of hydrodynamic screening (i.e., concentration-dependent change of the prefactor at large distances), known from unconfined systems, is fully confirmed by our experimental measurements as is seen in figure 2(e).

The first term in equation (19) represents the leading correction to equations (7) and (8) as the inter-particle distance ρ decreases. It scales as $h(\rho)/\rho^2$ and, therefore, should be in phase with the oscillations of the static pair correlation. The second term is smaller, of order $ah(\rho)/\rho^3$. Higher-order corrections, which have not been treated here, come from several sources. Corrections of $\mathrm{O}(a^2/\rho^4)$ arise from the integration in equation (18) (see the appendix), as well as the force–dipole terms (δv^s) discussed above. Terms of $\mathrm{O}(h^2/\rho^2)$ come from the approximation employed in equation (17). Finally, as ρ becomes comparable to w, short-distance hydrodynamics set in and the far flow (4), on which our entire analysis has been relying, should be corrected [18]. Thus, the expression formulated in equation (19) is relevant to suspensions of sufficiently high concentration, such that the static pair correlation $h(\rho)$ is significant at distances $\rho > w$ where the far flow holds.

To compare equation (19) with experiment we need the static pair correlation function for the various values of area fraction. These functions are directly measurable from snapshots of the Q2D suspensions such as the one shown in figure 1(a). (For more details, see [20].) The results are presented in figure 3.

The measured $h(\rho)$ are subsequently used in equation (19) to calculate the correction to the pair interaction. The results are shown in figure 4. With the coefficient λ of the bare interaction

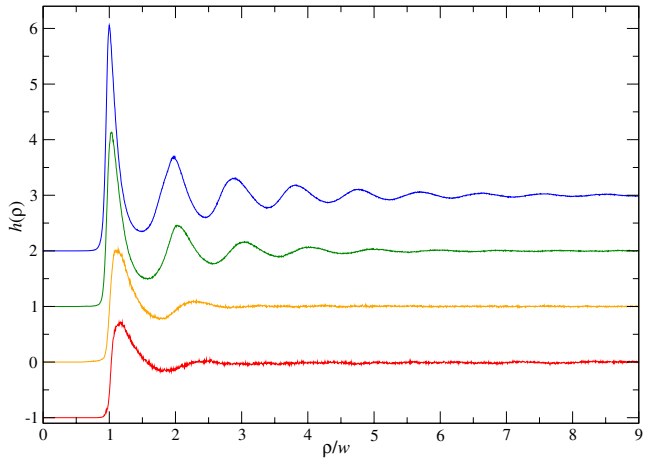

Figure 3. Static pair correlation function as measured from suspension snapshots. Plotted is $h(\rho) = g(\rho) - 1$, where $g(\rho)$ is the pair correlation function normalized to 1 at $\rho \to \infty$. The inter-particle distance is scaled by w. Area fractions are, from the bottom up, $\phi = 0.254$ (red), 0.338 (orange), 0.547 (green), and 0.619 (blue). Curves are vertically shifted by 1 for clarity.

already found, there is only one unknown coefficient, C, fitted as $C \simeq 0.85$. Substituting this value back in the definitions of the various coefficients introduced during the calculation, we find the coefficient of the third force moment for our experimental system ($a/w \simeq 0.45$) to be $\lambda_t \simeq 1.77$. Comparing the fits in figure 4 with those in figure 2, we see that the introduction of the concentration-dependent correction leads to a good agreement between the theory and the measured longitudinal interaction not only at asymptotically large distances (as was presented in [10, 11]) but also at intermediate distances, $\rho > 2w$. As anticipated, equation (19) is particularly successful for the high-concentration systems (figures 4(c) and (d)), where oscillations related to $h(\rho)$ are clearly observed (compare with figure 3). The discrepancies seen in figure 4 between the theory and experiment for $\rho \lesssim 2w$ can be attributed to several factors, as discussed above, which have not been included in the current analysis.

Our calculation has yielded an identical correction to the transverse pair interaction, $\delta\Delta_T = \delta\Delta_L$. This does not agree with the measured transverse interaction, which does not exhibit a wiggly behaviour similar to that of Δ_L (see figure 2). Thus, we cannot currently offer an accurate analysis of the concentration effect on the transverse interaction at intermediate and short distances. A possible reason for the difference between the longitudinal and transverse modes may lie in the higher sensitivity of the latter to short-range hydrodynamics. To demonstrate this difference we show in figure 5 the deviations of the longitudinal and transverse bare interactions from their large-distance behaviour in the limit of very small particles ($a/w \ll 1$), as obtained from an exact solution [18]. The departure of the transverse interaction from its asymptotic behaviour is found to be more pronounced than that of the longitudinal one.

7. Discussion

The correlated dynamics of particles in Q2D suspensions are very different from those in unconfined systems. Confinement affects the decay of the dynamic correlation with distance ($1/r^2$ instead of $1/r$) as well as its sign (the correlation transverse to the line connecting the particles becomes negative). In the current work we have focused on the effect of

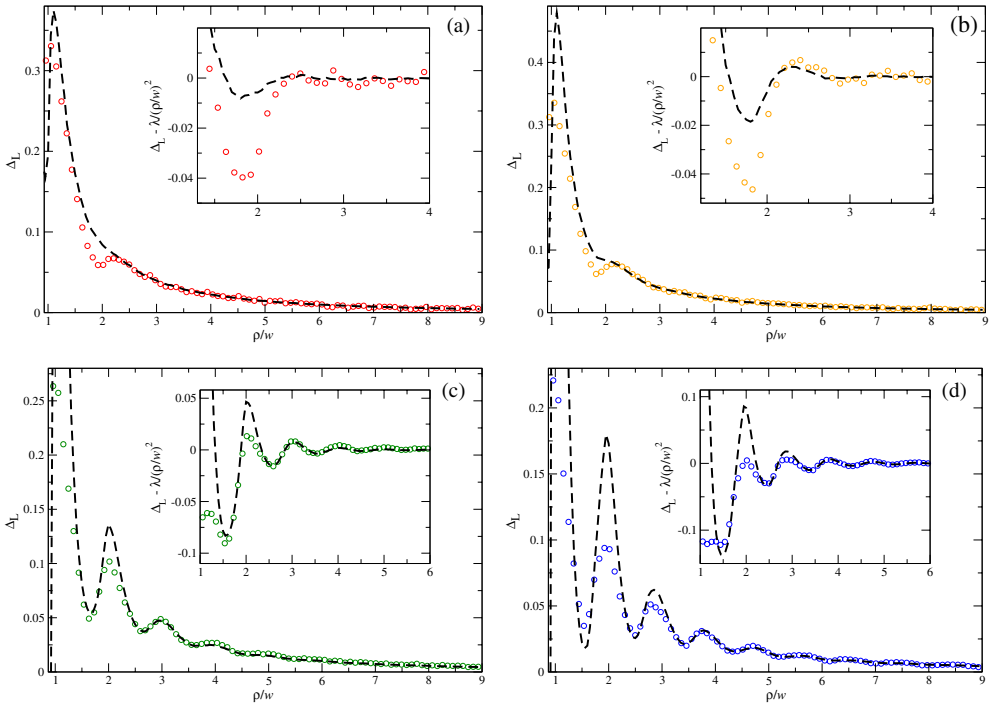

Figure 4. Concentration effect on the longitudinal coupling diffusion coefficient. The diffusion coefficient is scaled by $D_0 a/w$ and the inter-particle distance by w. Area fractions are $\phi = 0.254$ ((a), red), 0.338 ((b), orange), 0.547 ((c), green), and 0.619 ((d), blue). Dashed lines are a fit to equations (7), (19) with $\lambda = 0.36$ (already fitted in figure 2) and $C = 0.85$ for all panels. Insets focus on the deviation of the coupling from its long-distance behaviour. The oscillations at high concentration are in phase with those of the measured static pair correlation (see figure 3).

concentration, i.e., the presence of additional particles, on the pair interaction. Unlike unconfined suspensions, where the large-distance coupling changes with concentration, in Q2D suspensions increasing the concentration has no effect at large inter-particle distances (no hydrodynamic screening). The qualitatively different behaviour of Q2D suspensions has been theoretically and experimentally corroborated. It stems from the dipolar shape of the far flow induced by particle motion. As argued in [10, 11, 22], the key property of this flow is that it is governed by the displacement of liquid mass rather than the diffusion of liquid momentum.

Concentration-dependent effects on the pair correlation do set in in Q2D suspensions, yet only at intermediate and short distances. The range of these corrections is determined by the larger of two lengths: the range of the static pair correlation $h(\rho)$ of the suspension and the confinement width w. In the former case, which is valid for sufficiently high concentration, the spatial dependence of the dynamic coupling reflects the features of the static pair correlation. In this case we have been able to provide a quantitative account for the concentration effect on the longitudinal interaction at intermediate distances, which is in good agreement with the experimental measurements. In the latter case (range of h shorter than w), the correction depends on short-range hydrodynamics whose analysis lies beyond the scope of the current work.

We have not treated the effect of particle motion perpendicular to the bounding surfaces. Such fluctuations must exist in practice, yet our results suggest that they have a minor effect at

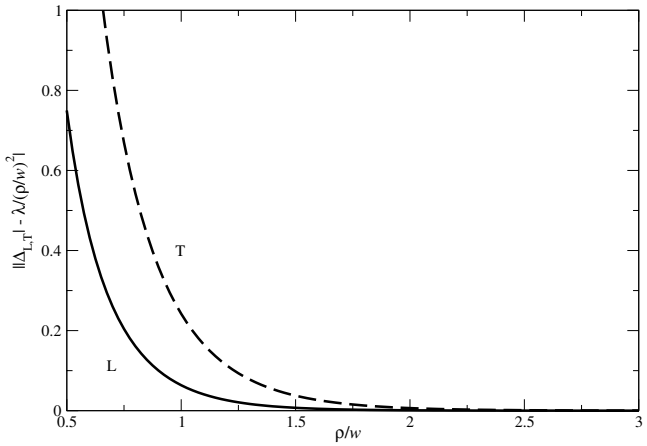

Figure 5. Deviation of the pair interaction from its large-distance behaviour in the limit of very small particles. The deviation of the transverse interaction (T, dashed line) is larger than that of the longitudinal one (L, solid line). The curves were calculated using the exact solution for $a/w \ll 1$ given in [18]. The large-distance behaviour in this limit is given by $\Delta_{\mathrm{L,T}} \simeq \pm\lambda/(\rho/w)^2$, with $\lambda = 9/16$.

large and intermediate distances. This is expected since the flows produced by perpendicular fluctuations decay exponentially with distance and thus have only a short-range effect [18].

Acknowledgments

This research was supported by the Israel Science Foundation (77/03), the National Science Foundation (CTS-021774 and CHE-9977841) and the NSF-funded MRSEC at The University of Chicago. HD acknowledges additional support from the Israeli Council of Higher Education (Alon Fellowship).

Appendix

We need to calculate the integral appearing in equation (18):

$$I(\boldsymbol{\rho}) = \int \mathrm{d}^2\rho'\,[1 + 2h(\rho')][\Delta_{xx}(\boldsymbol{\rho}')\Delta_{xx}(\boldsymbol{\rho} - \boldsymbol{\rho}') + \Delta_{xy}(\boldsymbol{\rho}')\Delta_{xy}(\boldsymbol{\rho} - \boldsymbol{\rho}')], \tag{20}$$

where (omitting the prefactor)

$$\Delta_{xx}(\boldsymbol{\rho}) = (x^2 - y^2)/\rho^4, \qquad \Delta_{xy}(\boldsymbol{\rho}) = 2xy/\rho^4. \tag{21}$$

Changing to polar coordinates, $\boldsymbol{\rho} = (\rho, \varphi)$ and $\boldsymbol{\rho}' = (\rho', \varphi')$, we rewrite the integral as

$$I(\boldsymbol{\rho}) = \int \mathrm{d}^2\rho'\,[1 + 2h(\rho')]\frac{\rho^2\cos[2(\varphi' - \varphi)] + \rho'^2 - 2\rho\rho'\cos(\varphi' - \varphi)}{\rho'^2[\rho^2 + \rho'^2 - 2\rho\rho'\cos(\varphi' - \varphi)]^2}, \tag{22}$$

from which it is evident that $I(\boldsymbol{\rho}) = I(\rho)$ is independent of φ. Hence, we may set $\varphi = 0$. This isotropy immediately implies also that the corrections to the longitudinal and transverse couplings, proportional to $I(\rho\hat{x})$ and $I(\rho\hat{y})$, respectively, are identical.

The calculation of $I(\boldsymbol{\rho})$ via equation (22) is a bit tricky for reasons similar to those encountered in electrostatics. We exclude two small areas $\sim a^2$ around the (integrable) singularities at $\rho' = 0$ and $\boldsymbol{\rho}' = \boldsymbol{\rho}$, and divide the integration into three domains:

(i) $\rho' \in (a, \rho - a)$, $\varphi' \in (0, 2\pi)$; (ii) $\rho' \in (\rho + a, \infty)$, $\varphi' \in (0, 2\pi)$; (iii) $\rho' \in (\rho - a, \rho + a)$, $\varphi' \in (a/\rho, 2\pi - a/\rho)$. The contribution from the inner domain (i) vanishes upon integration over φ' for any $\boldsymbol{\rho}$. (Note that the static pair correlation $h(\rho)$ does not have an angular dependence.) Integration over φ' in the outer domain (ii) gives $2\pi[1 + 2h(\rho')]/(\rho')^3$. Subsequent integration over ρ' in domain (ii) yields $2\pi \int_\rho^\infty \mathrm{d}\rho' [1 + 2h(\rho')]/(\rho')^3 + \mathrm{O}(a/\rho^3)$. However, due to the integrable singularity at $\boldsymbol{\rho}' = \boldsymbol{\rho}$, the intermediate narrow domain (iii) has a finite contribution as well, of opposite sign: $-\pi[1 + 2h(\rho)]/\rho^2 + \mathrm{O}(a/\rho^3)$.

Thus, in the absence of static correlations, $h(\rho) = 0$, the leading terms in small a/ρ from domains (ii) and (iii) cancel and $I(\rho \gg a) = 0$. This result has already been obtained in [10, 11]. A more detailed inspection reveals that the $\mathrm{O}(a/\rho^3)$ corrections from domains (ii) and (iii) cancel as well and, hence, $I = \mathrm{O}(a^2/\rho^4)$.

In the presence of static correlations, $h \neq 0$, we finally get

$$I(\boldsymbol{\rho}) = -2\pi \left[\frac{h(\rho)}{\rho^2} - 2 \int_\rho^\infty \mathrm{d}\xi \, \frac{h(\xi)}{\xi^3} \right] + \mathrm{O}(a^2/\rho^4). \tag{23}$$

References

[1] Russel W B, Saville D A and Schowalter W R 1989 *Colloidal Dispersions* (New York: Cambridge University Press)
[2] Doi M and Edwards S F 1986 *The Theory of Polymer Dynamics* (New York: Oxford University Press)
[3] Happel J and Brenner H 1973 *Low Reynolds Number Hydrodynamics* (The Hague: Martinus Nijhoff)
[4] Perkins G S and Jones R B 1992 *Physica* A **189** 447
[5] Dufresne E R, Squires T M, Brenner M P and Grier D G 2000 *Phys. Rev. Lett.* **85** 3317
[6] Lobry L and Ostrowsky N 1996 *Phys. Rev.* B **53** 12050
[7] Lin B, Yu J and Rice S A 2000 *Phys. Rev.* E **62** 3909
[8] Dufresne E R, Altman D and Grier D G 2001 *Europhys. Lett.* **53** 264
[9] Cui B, Diamant H and Lin B 2002 *Phys. Rev. Lett.* **89** 188302
[10] Cui B, Diamant H, Lin B and Rice S A 2004 *Phys. Rev. Lett.* **92** 258301
[11] Diamant H, Cui B, Lin B and Rice S A 2005 *J. Phys.: Condens. Matter* **17** S2787
[12] Xu X L and Rice S A 2005 *J. Chem. Phys.* **122** 024907
[13] Crocker J C and Grier D G 1996 *J. Colloid Interface Sci.* **179** 298
[14] Grier D G 1997 *Curr. Opin. Colloid Interface Sci.* **2** 264
[15] Pesche R and Nagele G 2000 *Europhys. Lett.* **51** 584
Pesche R and Nagele G 2000 *Phys. Rev.* E **62** 5432
[16] Zangi R and Rice S A 2004 *J. Phys. Chem.* B **108** 6856
[17] Chvoj Z, Lahtinen J M and Ala-Nissila T 2004 *J. Stat. Mech.* P11005
Falck E, Lahtinen J M, Vattulainen I and Ala-Nissila T 2004 *Eur. Phys. J.* E **13** 267
[18] Liron N and Mochon S 1976 *J. Eng. Math.* **10** 287
[19] Bhattacharya S and Blawzdziewicz J 2002 *J. Math. Phys.* **43** 5720
Bhattacharya S, Blawzdziewicz J and Wajnryb E 2005 *Preprint* cond-mat/0504697
Bhattacharya S, Blawzdziewicz J and Wajnryb E 2005 *Preprint* cond-mat/0504699
[20] Cui B, Lin B and Rice S A 2001 *J. Chem. Phys.* **114** 9142
[21] Cui B, Lin B, Sharma S and Rice S A 2002 *J. Chem. Phys.* **116** 3119
[22] Ramaswamy S 2001 *Adv. Phys.* **50** 297
[23] Long D, Stone H A and Ajdari A 1999 *J. Colloid Interface Sci.* **212** 338
Long D and Ajdari A 2001 *Eur. Phys. J.* E **4** 29